# Topological singularities of domains in globally constrained bistable reaction-diffusion systems

Baruch Meerson and Igor Mitkov
*Racah Institute of Physics, Hebrew University of Jerusalem, Jerusalem 91904, Israel*
(Received 30 April 1996)

A general (nonvariational) globally constrained reaction-diffusion equation (GCRDE) with bistability is employed for studying the dynamics of two-dimensional non-single-connected domains: circular spots of one phase with inclusions of another phase. In the sharp-interface approximation, the dynamics is describable by a set of coupled ordinary differential equations which have a universal form. It is shown that domains with a single inclusion always develop topological singularity in a finite time: the inclusion either shrinks to zero, or breaks out. The results are supported by numerical simulations with the full GCRDE.
[S1063-651X(96)02311-2]

PACS number(s): 82.40.Ck, 82.20.Mj

Bistable reaction-diffusion systems with global constraints are probably the simplest continuous systems showing two-phase segregation, coexistence [1,2], and coarsening [3–5], and they have appeared in various applications (electrothermal domains in semiconductors, metals, and superconductors [6], thermal contraction in weakly ionized plasmas [7], bistable heterogeneous chemical reactions [8], radiative condensations in optically thin plasmas [9,10], etc). In spite of their simplicity, these systems can have quite a rich dynamics, as they cannot be reduced, in general, to a gradient flow. The most transparent evidence for this nonvariational behavior is the limit-cycle-type domain dynamics that were experimentally observed and theoretically interpreted in recent years [6,11]. Also, it has been found recently [5] that, under quite general conditions, the dynamics of a large number of simple domains (''spots''), as described by a general globally constrained reaction-diffusion equation (GCRDE) with bistability, can be mapped into a mean-field model of Ostwald ripening (OR) [12–14]. In contrast to the ''conventional'' mean-field models of OR, this particular model is ''almost exact,'' as it does not require a small volume or area fraction [5]. In this paper we report on another interesting property of the GCRDE with bistability: topological singularities that develop in non-single-connected domains (spots of one phase with inclusions of the other phase).

Consider a reaction-diffusion equation for a scalar order parameter $u(\mathbf{r},t)$ in a scaled form:

$$\frac{\partial u}{\partial t}=\nabla^2 u+f(u,p). \tag{1}$$

Here $p(t)$ is an additional, ''global'' parameter (inhibitor). In the case of bistability, the function $f(u,p)$ has, at fixed $p$, three zeros, $u_1(p)<u_u(p)<u_2(p)$, such that $\partial f/\partial u<0$ for $u=u_{1,2}$ (locally stable phases 1 and 2) and $>0$ for $u=u_u$ (unstable phase). The dynamics of the inhibitor is governed by a global constraint,

$$\int_\Omega K[u(\mathbf{r},t),p(t)]d\mathbf{r}=\text{const}\ . \tag{2}$$

The problem is defined on a finite planar domain $\Omega$, the area of which is $S$. Equation (2), introduced in Ref. [5], generalizes a number of previously employed global constraints (such as constant voltage, constant average temperature, mass conservation, etc.). Complemented with initial and boundary conditions, Eqs. (1) and (2) represent a closed set.

Assume for simplicity that none of the functions $f$ and $K$ nor their derivatives introduce any small or large parameters, and that all characteristic domain sizes are much larger than the width of the interphase boundary (which is of order unity). Let there exist a special value of the inhibitor, $p=p_*$, for which the area rule,

$$\int_{u_1(p)}^{u_2(p)} f(u,p)du=0\,, \tag{3}$$

holds. For $p=p_*$, a planar interface, separating the regions of the phase 1 and phase 2 [with the order parameter values $U_{1,2}=u_{1,2}(p_*)$], would be in equilibrium (see, e.g., [1,2]). When $p$ deviates from $p_*$ and/or the interface is curved, the domains will either shrink or expand. We assume that the globally constrained two-phase coexistence is stable with respect to the fast mode instability [6,11] (which, when it develops, typically has a growth rate of order unity). The corresponding condition (so-called Elmer's inequalities) imposes certain limitations on the functions $f$ and $K$ and their partial derivatives with respect to $u$ and $p$.

Let $\mathbf{n}$ be the normal to the interface directed from phase 1 to phase 2. The (slowly time-varying) normal interface speed is given by

$$c_n(t)=-g\,\delta p(t)-\mathcal{K}(t), \tag{4}$$

where the inhibitor mismatch $\delta p=p-p_*$ is assumed to be small, and $g$ is a numerical factor of order unity that can be calculated analytically once the function $f(u,p)$ is known [1]. In addition, $\mathcal{K}$ is the (small) local curvature of the interface, defined to be positive if the interface is convex towards phase 2 and negative otherwise.

The dynamics of a small inhibitor mismatch $\delta p$ is governed by the following relation [5]:

 

$$\frac{d\,\delta p}{dt}=-\left(\delta p+\frac{\langle\mathcal{K}\rangle}{g}\right)\frac{g\Lambda[K(U_2,p_*)-K(U_1,p_*)]}{S_1\left.\frac{dK}{dp_*}\right|_1+S_2\left.\frac{dK}{dp_*}\right|_2}, \quad (5)$$

where $S_{1,2}$ are the total areas of phases 1 and 2 ($S_1+S_2=S$), $\Lambda$ is the total length of the interfaces between the two phases, $\langle\,\rangle$ means averaging over all interfaces, and

$$\left.\frac{dK}{dp_*}\right|_{1,2}=\left.\frac{\partial K}{\partial p_*}\right|_{u=U_{1,2}}+\left.\frac{\partial K}{\partial u}\right|_{u=U_{1,2}}\frac{du_{1,2}}{dp_*}.$$

The sharp-interface equations (4) and (5) were employed in Ref. [5] to solve analytically a number of model problems of stability of and competition between single-connected domains. In the following we shall use both the sharp-interface equations and the full system of Eqs. (1) and (2) to analyze the dynamics of non-single-connected domains. We shall see that these dynamics look quite different.

Consider a single circular spot of, say, phase 1 with $N$ circular inclusions of phase 2. The circular-interface model is justified in view of stability of a circular interface with respect to azimuthal deformations [5]. Let the spot radius be $R$, and the inclusion radii be $r_i<R$, $i=1,2,\ldots,N$. Assume that $\delta p$ is sufficiently small, and all $r_i\gg 1$, so that we can use the sharp-interface equations (4) and (5). We immediately arrive at the following set of ordinary differential equations:

$$\dot{R}=-g\,\delta p-\frac{1}{R}, \quad (6)$$

$$\dot{r}_i=g\,\delta p-\frac{1}{r_i}, \quad i=1,2,\ldots,N \quad (7)$$

$$\delta\dot{p}=-\epsilon g\,\delta p\left(R+\sum_{i=1}^{N}r_i\right)+\epsilon(N-1), \quad (8)$$

where

$$\epsilon=\frac{2\pi[K(U_2,p_*)-K(U_1,p_*)]}{S(dK/dp_*)|_2},$$

and we have assumed for simplicity that $\pi R^2\ll S$. Notice that the averaged curvature $\langle\mathcal{K}\rangle$ vanishes and does not contribute to Eq. (8) in the case of $N=1$ (a single inclusion). Particular forms of functions $f$ and $K$ enter Eqs. (6)–(8) only through the factors $g$ and $\epsilon$. Furthermore, these factors can be eliminated altogether if we introduce scaled variables, $\tilde{R}=(\epsilon g)^{1/3}R$, $\tilde{r}=(\epsilon g)^{1/3}r$, and $P=\epsilon^{-1/3}g^{2/3}\delta p$, and scaled time $\tilde{t}=(\epsilon g)^{2/3}t$. As the result, the governing equations take a universal form:

$$\dot{R}=-P-\frac{1}{R}, \quad (9)$$

$$\dot{r}_i=P-\frac{1}{r_i}, \quad i=1,2,\ldots,N \quad (10)$$

$$\dot{P}=-P\left(R+\sum_{i=1}^{N}r_i\right)+N-1\,, \quad (11)$$

where we have omitted all tildes. Equations (9)–(11) have the following first integral:

$$P-\frac{1}{2}\left(R^2-\sum_{i=1}^{N}r_i^2\right)=C=\text{const}\ . \quad (12)$$

In what follows we consider the dynamics of a spot with a single inclusion of a radius $r$. In this case, instead of $N$ equations (10), we have a single equation

$$\dot{r}=P-\frac{1}{r}, \quad (13)$$

Equation (11) becomes

$$\dot{P}=-P(R+r), \quad (14)$$

while the first integral (12) takes the form

$$P-\frac{1}{2}(R^2-r^2)=C=\text{const}. \quad (15)$$

The inclusion of phase 2 is, in general, nonconcentric with the spot, and we shall denote the scaled eccentricity (the intercenter distance between the spot and the inclusion) $d$. It is seen from Eqs. (9) and (13) that a non-single-connected domain cannot be in equilibrium. Furthermore, topological singularity always develops in a finite time. The first type of singularity corresponds to the inclusion shrinking to zero, $r\to 0$. The second one can be called reconnection, and it occurs when the difference of the radii $R-r$ becomes equal to the (invariable) eccentricity $d$. In both cases, the domain becomes single connected after singularity.

To clarify the matter, let us start with the simplest case of $P(t=0)=P_0=0$ (that corresponds to the area-rule value $p=p_*$), when a simple analytic solution of Eqs. (9), (13), and (14) is available. It follows from Eq. (14) that $P$ remains zero for all $t>0$, and Eqs. (9) and (13) are immediately solved. Both the spot radius $R$ and the inclusion radius $r$ decrease with time, and the inclusion radius reaches zero first:

$$r(t)=r_0(1-t/t_s)^{1/2},$$

where $t_s=r_0^2/2$ is the shrinkage time, and $r_0=r(t=0)$. Up to the shrinkage time $t_s$, the spot radius $R$ behaves like

$$R(t)=R_0[1-2t/R_0^2]^{1/2}$$

[where $R_0=R(t=0)$]. For $t>t_s$ Eqs. (13) and (14) are not applicable anymore. As topology changes and the spot becomes single connected, one should again employ Eq. (5) to get a new equation for $\dot{P}$. In the same scaled variables, this equation is the following:

$$\dot{P}=-PR-1, \quad (16)$$

which, combined with Eq. (9), determines the further evolution of the single-connected spot [5]. The first integral becomes simply

$$P-\frac{R^2}{2}=\text{const} \tag{17}$$

and the problem is integrable. Depending on $R_0$, the remnant spot either shrinks to zero or approaches a stable equilibrium with a finite value of $R$.

Now let us consider a nonzero $P_0$. It follows from Eq. (14) that $|P|$ decreases with time, while the sign of $P$ does not change. It is easy to see that, if $P_0$ is negative, the inclusion always shrinks to zero. Indeed, $P$ remains negative for all $t$ [see Eq. (14)], and the right-hand side of Eq. (13) is always negative and larger by the absolute value than the right hand side of Eq. (9). The shrinkage to zero always develops in a finite time $t_s$ (which, for the same $R_0$, is smaller than its value for $P=0$). Near the singularity, the $-1/r$ term in Eq. (13) dominates, so that the leading term in the asymptotics of $r(t)$ near $t=t_s$ is $[2(t_s-t)]^{1/2}$. At $t=t_s$, the spot becomes single connected, and its further evolution proceeds according to the sharp-interface equations (9), (16), and (17).

The case of a positive $P_0$ is more complicated, as singularities of both types are possible, depending, in addition, on the eccentricity $d$ and on the initial values of the radii. We found two sufficient conditions, one for shrinkage to zero and one for reconnection, in terms of the value of the first integral $C$ [see Eq. (15)]. First, if $C<C_1=-(1/2)d(R_0+r_0)$, shrinkage always occurs. This can be proved in the following way. Introduce the reconnection parameter $\eta=R-r-d\geqslant 0$, so that $\eta=0$ corresponds to reconnection. The first integral (15) can be rewritten as

$$C=P-\frac{1}{2}(d+\eta)(R+r).$$

For $P>0$ and $C<C_1$ the double inequality

$$-\frac{1}{2}(d+\eta)(R+r)<C<C_1$$

holds. It follows that

$$(R+r)\,\eta>d[R_0+r_0-(R+r)].$$

Now, the sum of the radii, $R+r$, always decreases in time [it can be checked by adding up Eqs. (9) and (13)]; therefore the right hand side of the last inequality is positive for all $t>0$. It follows that $\eta$ remains positive, and no reconnection is possible, which means shrinkage to zero.

On the other hand, if $C>C_2$, where

$$C_2=\frac{1}{r_0}-\frac{d(2r_0+d)}{2},$$

then reconnection always occurs. To prove it, we first prove that $C>C_2$ implies $P_0>1/r_0$, so that $r(t)$ increases in time (at least, initially). Indeed, the inequality $C>C_2$ can be rewritten as

$$P_0>\frac{1}{r_0}+\frac{1}{2}(R_0^2-r_0^2-2dr_0-d^2),$$

which, combined with $R_0-r_0-d>0$, leads to $P_0>1/r_0$. This means that $r(t)$ increases monotonically, so that reconnection is inevitable (remember that $R+r$ decreases with time).

One might think of another possibility: there might be a moment of time $t_*$ for which $r(t)$ reaches its maximum value $r_*$ before reconnection. In fact, this possibility does not exist: reconnection occurs before $r(t)$ can reach its maximum. Indeed, a maximum for $r(t)$ would mean that $P_*=1/r_*$ at $t=t_*$ [see Eq. (13)]. Obviously, in this case $1/r_*$ must be less than $1/r_0$. On the other hand, if there is no reconnection, then $R_*-r_*-d>0$ and we have

$$\begin{aligned}\frac{1}{r_*}=P_*&=C+\frac{1}{2}({R_*}^2-{r_*}^2)>C+\frac{1}{2}d(R_*+r_*)>C\\&\quad+\frac{1}{2}d(2r_*+d)>C+\frac{1}{2}d(2r_0+d)\\&=C-C_2+\frac{1}{r_0}.\end{aligned}$$

Since $C>C_2$, we arrive at $1/r_*>1/r_0$, which contradicts our assumption. Therefore $C>C_2$ indeed represents a sufficient condition for reconnection.

We can reformulate these two criteria in the following way. Introduce

$$P_1=\frac{1}{2}(R_0+r_0)(R_0-r_0-d) \tag{18}$$

and

$$P_2=\frac{1}{r_0}+\frac{1}{2}(R_0+r_0+d)(R_0-r_0-d). \tag{19}$$

Obviously, $0<P_1<P_2$. Then shrinkage to zero always occurs for $P_0<P_1$, while reconnection always occurs for $P_0>P_2$. Our numerical simulations with the sharp-interface equations (9), (13), and (14) show that a critical value $P_c$ exists somewhere between $P_1$ and $P_2$, so that inequality $P_0<P_c$ ($P_0>P_c$) represents the necessary and sufficient condition for shrinkage to zero (reconnection).

Close to a singularity, the sharp-interface theory breaks down. Therefore we performed numerical simulations with the full model equations (1) and (2). For the simulations we chose

$$f(u,p)=-(u-1)\left(u-\frac{1}{p}\right)(u-3) \tag{20}$$

and $K(u,p)=up$. Then Eq. (2) yields an explicit equation for $p(t)$:

$$p(t)=p(0)\frac{\int_\Omega u(\mathbf{r},0)d\mathbf{r}}{\int_\Omega u(\mathbf{r},t)d\mathbf{r}}. \tag{21}$$

Also, for this choice of $f$ and $K$ one obtains $p_*=1/2$, $g=4\sqrt{2}$, and $\epsilon=2\pi/3S$. One can check that the Elmer inequalities [11,5] are satisfied in this case, so that the fast mode instability is suppressed. In addition, the theory of

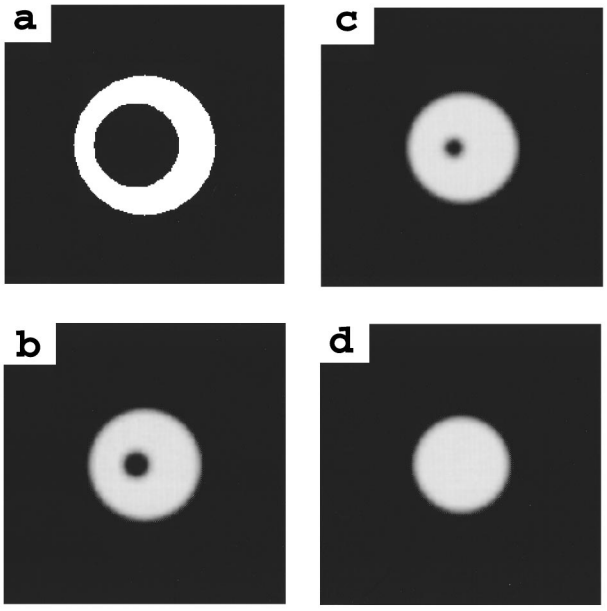


FIG. 1. Simulation results for the time evolution of the field $u(x,y)$ in the case of the inclusion shrinking to zero. The box size is $100\times100$, the number of grid points is $257\times257$. The initial values of the spot and inclusion radii and eccentricity are 25, 15, and 3, respectively, while $p(0)=0.5$. Snapshots $a$, $b$, $c$, and $d$ correspond to $t=0$, 105, 109, and 400, respectively.

Ref. [5] predicts stability of a planar interface, so that the long-time dynamics is affected by the interface curvature.

For the simulations we used a technique described in the Appendix. Typical simulation results are shown in Figs. 1–4. The initial conditions represented a non-single-connected domain with a single inclusion and nonconcentric circular boundaries. Figures 1 and 2 refer to the case of $p(0)=p_*=0.5$ (area-rule value). In this case the sharp-interface theory predicts shrinkage of the inclusion to zero under a constant $p$, followed by the evolution of the single-connected remnant domain according to Eqs. (16) and (17). Figure 1 shows the evolution of the $u$ field and indeed demonstrates shrinkage of the inclusion to zero. In Fig. 2 are shown theoretical and numerical results for $p(t)$. Until the shrinkage time, $p$ remains very close to 0.5, as predicted.

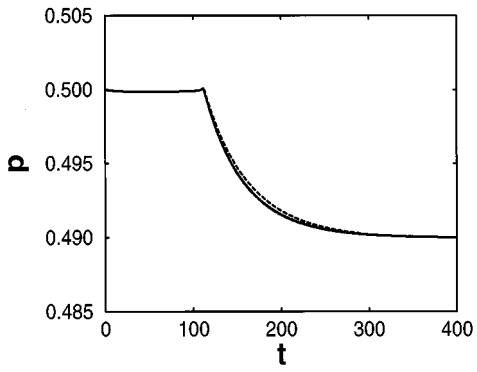


FIG. 2. Graphs of $p$ versus time in the case of the inclusion shrinking to zero. The solid line represents the result of simulations shown in Fig. 1. The dashed line is the prediction of the sharp-interface theory.

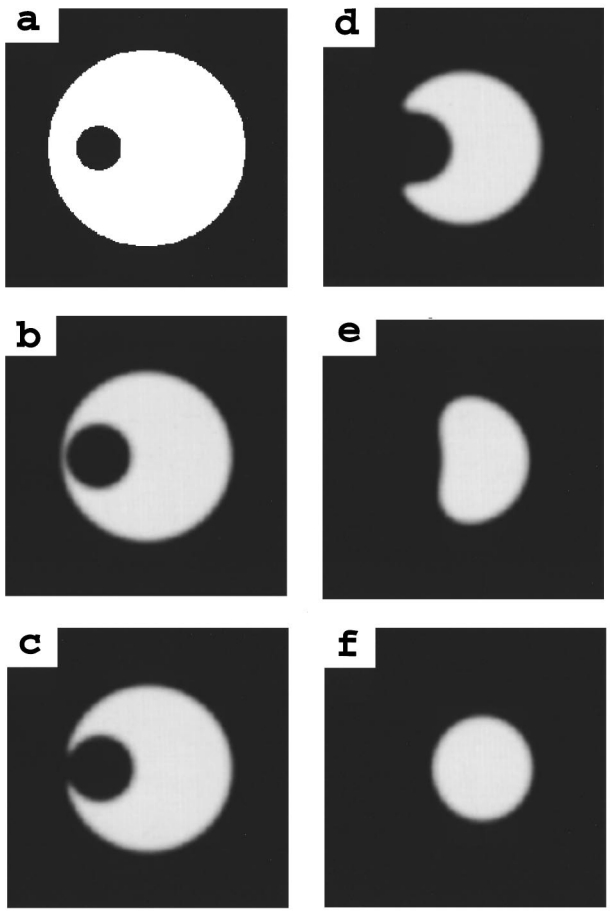


FIG. 3. Simulation results for the time evolution of the field $u(x,y)$ in the case of reconnection. The box size and grid are the same as in Fig. 1. The initial values of the spot and inclusion radii and eccentricity are 35, 8, and 17, respectively, while $p(0)=0.6$. Snapshots $a$, $b$, $c$, $d$, $e$, and $f$ correspond to $t=0$, 11.5, 13.5, 25, 95, and 350, respectively.

The small peak near the shrinkage time is not described by the sharp-interface theory, which becomes inapplicable here. After the shrinkage, there is only a single-connected circular spot left. The solution of the sharp-interface equations (16) and (17) (dashed curve) is in a good agreement with the

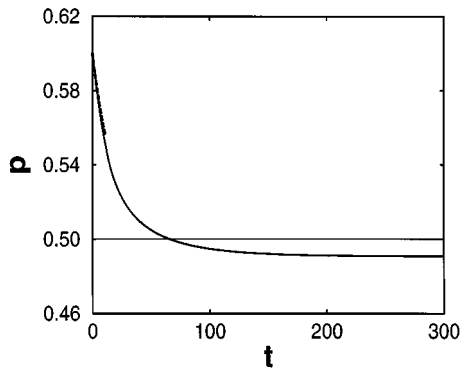


FIG. 4. Graphs of $p$ versus time in the case of reconnection. The solid line represents the result of simulations shown in Fig. 3. The dashed line is the prediction of the sharp-interface theory until the time of reconnection.

simulation results (solid curve), as the spot is approaching a stable equilibrium.

Figure 3 shows the evolution of the $u$ field for a different initial condition for $p$ which corresponds (according to our sufficient condition $P_0 > P_2$) to reconnection. Figure 3 demonstrates that reconnection indeed occurs, and it is followed by symmetrization of the spot and relaxation to a stable circular-spot equilibrium. Figure 4 shows the corresponding numerical (solid line) and theoretical (dashed line) curves for $p(t)$. The theoretical curve represents the solution of Eqs. (9), (13), and (14), and it describes the dynamics very well until the time of reconnection. After the reconnection the remnant spot boundary is not circular anymore, and the sharp-interface equations are insufficient for describing the dynamics (until the spot shape becomes close to circular again).

Possible experiments on the topological singularities include the systems the reduced dynamics of which are describable by the GCRDE. Schimansky-Geier *et al.* [3] give examples of thermokinetic systems with bistable behavior of concentration $n$, inhibited by temperature $T$ (like magnetic superconductors, where first-order phase transition to the ferromagnetic phase at low temperatures destroys superconductivity). If the temperature variable $T$ is fast, it becomes enslaved by the concentration. It turns out that the relation between $T$ and $n$ in this situation is nonlocal [3], which represents a particular case of global constraint (2).

In summary, we have employed the sharp-interface equations to study the dynamics of two-dimensional non-single-connected domains in a nonvariational GCRDE. We have found and analyzed analytically and numerically the topological singularities developing in domains with a single inclusion. The sharp-interface theory correctly predicts the type of singularity (shrinkage of the inclusion to zero, or reconnection) and gives a complete description of the dynamics until the time of singularity. In the case of shrinkage to zero, the sharp-interface theory describes essentially the whole dynamics, including the relaxation of the single-connected remnant spot to a stable equilibrium.

We acknowledge a useful discussion with L. Friedland. This research was supported in part by a grant from the Israel Science Foundation.

## APPENDIX

The simulations with the system (1), (21) were performed in the following way. Equation (1) was solved using an implicit pseudospectral approach. Consider a square box on a two-dimensional square grid, with the $u$ field defined at the sites of the grid. We chose the no-flux boundary condition $(\nabla u)_n = 0$. The $u$ field on the grid is transformed into the Fourier space, so that the partial differential equation (1) for $u(x,y,t)$ is replaced by a set of ordinary differential equations for its Fourier harmonics $\overline{u_{k_x,k_y}}$:

$$\frac{\partial \overline{u_{k_x,k_y}}}{\partial t} = -(k_x^2 + k_y^2 + 3)\overline{u_{k_x,k_y}} + \overline{w_{k_x,k_y}}, \tag{A1}$$

where we have separated the time-independent part of the linear term of the polynomial $f(u,p)$ [see Eq. (20)]: $f(u,p) = -3u + w(u,p)$.

The solution of Eq. (A1) on the interval $(t; t+\Delta t)$ can be formally written as

$$\overline{u_{k_x,k_y}}(t+\Delta t) = e^{-(k_x^2+k_y^2+3)\Delta t}\left[\overline{u_{k_x,k_y}}(t) + \int_t^{t+\Delta t} dt' \times \overline{w_{k_x,k_y}}(t') e^{(k_x^2+k_y^2+3)(t'-t)}\right].$$

For small $\Delta t$ we can rewrite it in the trapezoid approximation:

$$\overline{u_{k_x,k_y}}(t+\Delta t) = e^{-(k_x^2+k_y^2+3)\Delta t}\left[\overline{u_{k_x,k_y}}(t) + \frac{\Delta t}{2}\overline{w_{k_x,k_y}}(t)\right] + \frac{\Delta t}{2}\overline{w_{k_x,k_y}}(t+\Delta t). \tag{A2}$$

Let us define a new function $v = u - (\Delta t/2)w$. Then the implicit scheme (A2) takes the form

$$\overline{v_k}(t+\Delta t) = e^{-(k_x^2+k_y^2+3)\Delta t}[2\overline{u_k}(t) - \overline{v_k}(t)]. \tag{A3}$$

Therefore, in order to find $u(t+\Delta t)$, one has to calculate $\overline{u(t)}$ and $\overline{v(t)}$ [the Fourier transforms of $u(t)$ and $v(t)$, respectively], then calculate $\overline{v(t+\Delta t)}$ using Eq. (A3), return to the real space, and finally find $u(t+\Delta t)$ as a solution of the following algebraic equation:

$$v - u + \frac{\Delta t}{2} w(u) = 0\,. \tag{A4}$$

By virtue of the small value of $\Delta t$, we are interested in the root for which a relation $u = v + O(\Delta t)$ holds. Since Eq. (A4) is a cubic equation, this root can be found explicitly. The Fourier transformations were performed by a real cos-FFT (fast Fourier transform) routine in view of the no-flux boundary conditions, while $p(t)$ was advanced according to a discretized version of Eq. (21).

[1] A.S. Mikhailov, *Foundations of Synergetics I. Distributed Active Systems* (Springer-Verlag, Berlin, 1990).

[2] J.D. Murray, *Mathematical Biology* (Springer-Verlag, Berlin, 1989), p. 481.

[3] L. Schimansky-Geier, Ch. Zülicke, and E. Schöll, Z. Phys. B **84**, 433 (1991).

[4] J. Rubinstein and P. Sternberg, IMA J. Appl. Math. **48**, 249 (1992).

[5] B. Meerson and P.V. Sasorov, Phys. Rev. E **53**, 3491 (1996).

[6] A.Vl. Gurevich and R.G. Mints, Rev. Mod. Phys. **59**, 941 (1987).

[7] A.V. Nedospasov and V.D. Khait, *Oscillations and Instabili-*

*ties in Low-Temperature Plasmas* (Nauka, Moscow, 1979), p. 116.
[8] L. Pismen, Chem. Eng. Sci. **34**, 563 (1979).
[9] I. Aranson, B. Meerson, and P.V. Sasorov, Phys. Rev. E **47**, 4337 (1993); **52**, 948 (1995).
[10] B. Meerson, Rev. Mod. Phys. **68**, 215 (1996).
[11] F.-J. Elmer, Phys. Rev. A **41**, 4174 (1990).
[12] I.M. Lifshitz and V.V. Slezov, Zh. Éksp. Teor. Fiz. **35**, 479 (1958) [Sov. Phys. JETP **8**, 331 (1959)].
[13] C. Wagner, Z. Electrochem. **65**, 581 (1961).
[14] V.V. Slezov and V.V. Sagalovich, Usp. Fiz. Nauk. **151**, 67 (1987) [Sov. Phys. Usp. **30**, 23 (1987)].